The structure of heavy and superheavy nuclei with an assesment of theoretical uncertainties.

Anatoli Afanasjev
Mississippi State University

1. Motivation and introduction
2. Reexaming shell structure in covariant density functional theory
3. Confronting experimental data
4. Uncertainties in predictions of fission barriers
5. Conclusions

In collaboration with S. Abgemava (MSU), P. Ring (TU Munich), T. Nakatsukasa (Tsukuba U), H. Abusara (MSU) and E. Litvinova (West Michigan U)

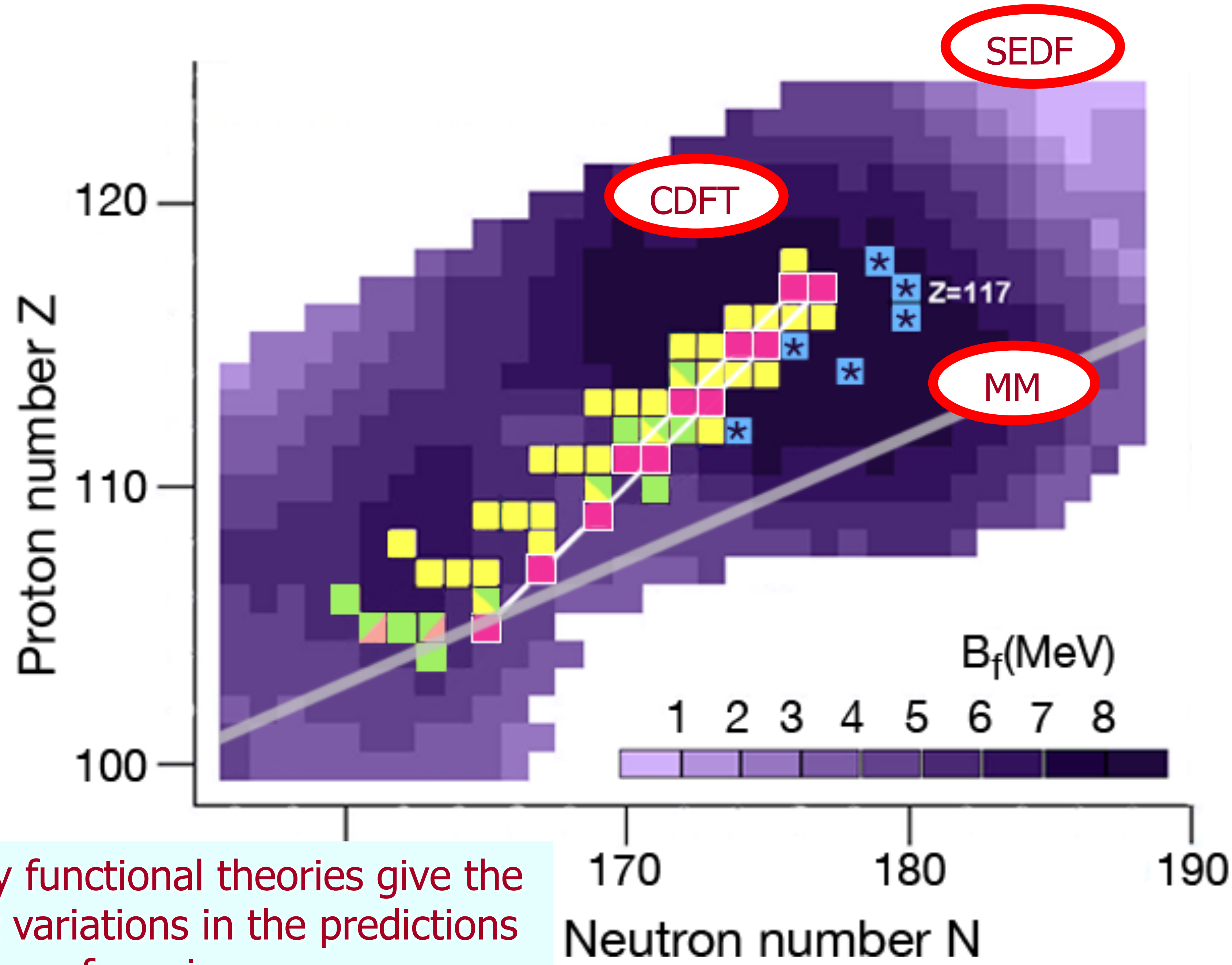

Density functional theories give the largest variations in the predictions of magic gaps

at Z=120, 126 and 172, 184

Covariant density functional theory (CDFT)

The nucleons interact via the exchange of effective mesons →

→ **effective Lagrangian**

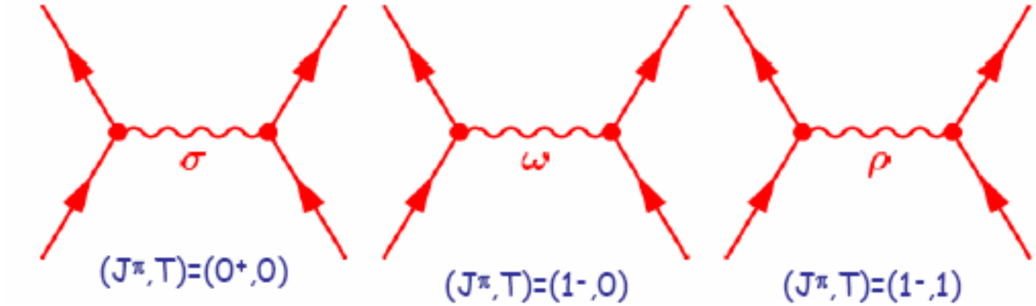

Long-range attractive scalar field	Short-range repulsive vector field	Isovector field

$$E_{\mathrm{RMF}}[\hat{\rho}, \phi_m] = \mathrm{Tr}[(\boldsymbol{\alpha p} + \beta m)\hat{\rho}] \pm \int \left[\frac{1}{2}(\nabla\phi_m)^2 + U(\phi_m)\right] \mathrm{d}^3 r + \mathrm{Tr}[(\Gamma_m \phi_m)\hat{\rho}]$$

density matrix $\hat{\rho}$ $\quad \phi_m \equiv \{\sigma, \omega^\mu, \vec{\rho}^\mu, A^\mu\}$ - meson fields

$$\hat{h} = \frac{\delta E}{\delta \hat{\rho}}$$ **Mean field**

$$\hat{h}|\varphi_i\rangle = \varepsilon_i |\varphi_i\rangle$$ **Eigenfunctions**

Two major differences between the state-of-the-art classes of covariant energy density functionals:

1. **Range of interaction (finite => mesons are included)**
   (zero => no meson, point-coupling models)

2. **Effective density dependence**
   - non-linear (through the power of sigma-meson)
   - explicit

Fitting protocol - another source of theoretical uncertainties in the definition of the functionals

All deformed calculations presented here for the ground states were obtained in axial Relativistic Hartree-Bogoliubov (RHB) framework with separable pairing (see S. Agbemava et al, PRC 92, 054310 (2015)).

Basic structure of CEDFs and their density dependence

The basic idea comes from ab initio calculations.
Density dependent coupling constants include
Brueckner correlations and three-body forces

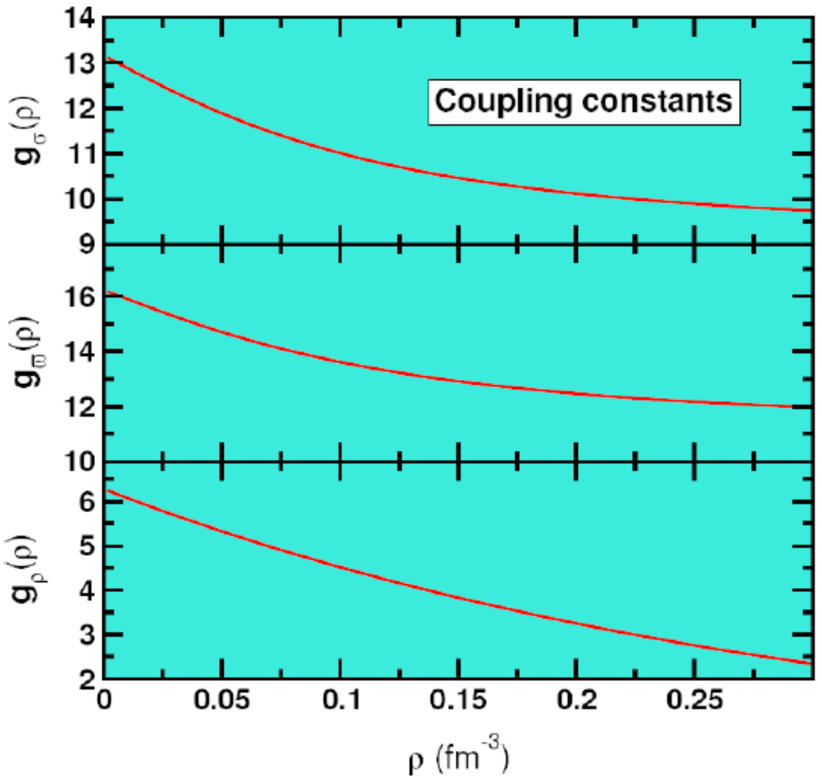

Effective interactions with medium-dependent couplings:

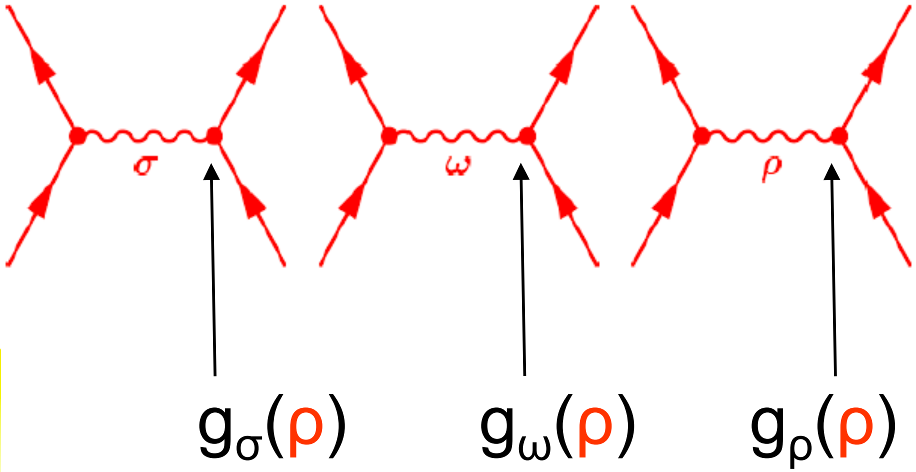

Remove mesons → point coupling models with derivative terms

Meson-exchange models

$$\mathcal{L} = \bar{\psi}[\gamma(i\partial - g_\omega \omega - g_\rho \vec{\rho}\,\vec{\tau} - eA) - m - g_\sigma \sigma]\psi$$
$$+ \frac{1}{2}(\partial\sigma)^2 - \frac{1}{2}m_\sigma^2\sigma^2 - \frac{1}{4}\Omega_{\mu\nu}\Omega^{\mu\nu} + \frac{1}{2}m_\omega^2\omega^2$$
$$- \frac{1}{4}\vec{R}_{\mu\nu}\vec{R}^{\mu\nu} + \frac{1}{2}m_\rho^2\vec{\rho}^{\,2} - \frac{1}{4}F_{\mu\nu}F^{\mu\nu},$$

Non-linear models

$$U(\sigma) = \frac{1}{2}m_\sigma^2\sigma^2 + \frac{1}{3}g_2\sigma^3 + \frac{1}{4}g_3\sigma^4$$

NL3*

Models with explicit density dependence

no nonlinear terms in the *σ meson*

$$g_i(\rho) = g_i(\rho_{\rm sat}) f_i(x) \quad \text{for} \quad i = \sigma, \omega, \rho$$

$$f_i(x) = a_i \frac{1 + b_i(x + d_i)^2}{1 + c_i(x + d_i)^2} \quad \text{for } \sigma \text{ and } \omega$$

$$f_\rho(x) = \exp[-a_\rho(x - 1)] \quad \text{for } \rho$$

$$x = \rho / \rho_{sat}$$

DD-ME2, DD-MEδ

Systematic Errors versus uncertainties:

systematic errors – well defined for the regions where experimental data exist [remember “error is a deviation from true value” (webster)]

theoretical uncertainties - not well defined for the regions beyond experimentally known

A. based on the set of the models which does not form statistical ensemble
B. biases of the models are not known
C. biases of the fitting protocols

Theoretical uncertainties are defined by the **spread** (the difference between maximum and minimum values of physical observable obtained with employed set of CEDF’s).

$$\Delta O(Z,N) = |O_{\max}(Z,N) - O_{\min}(Z,N)|$$

NL3*, DD-ME2, DD-MEδ, DD-PC1 [also PC-PK1 in superheavy nuclei]

Systematic errors in the description of masses

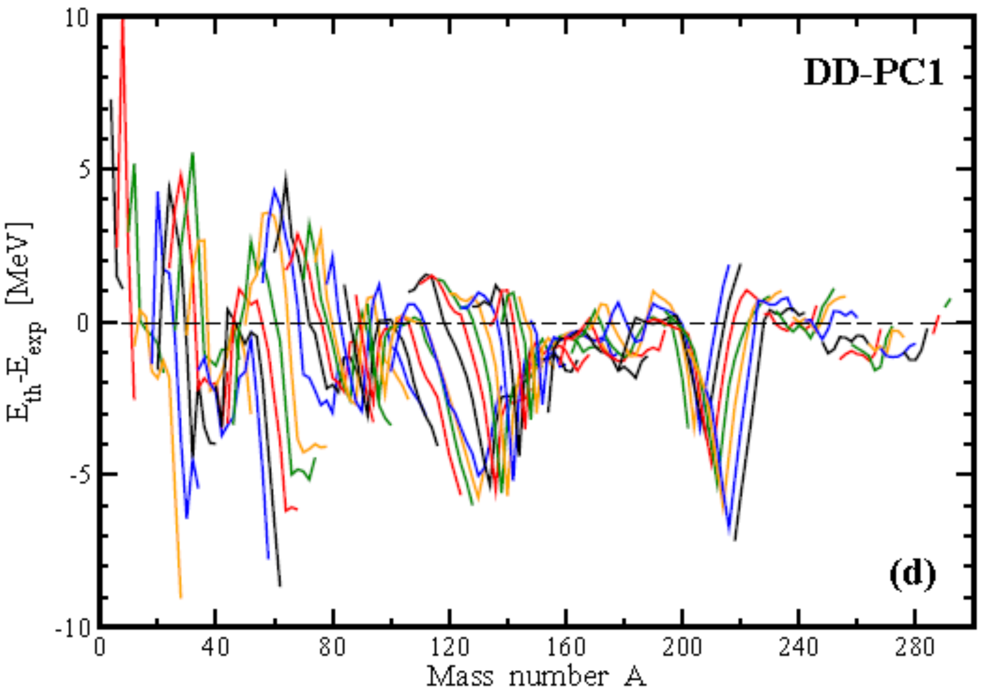

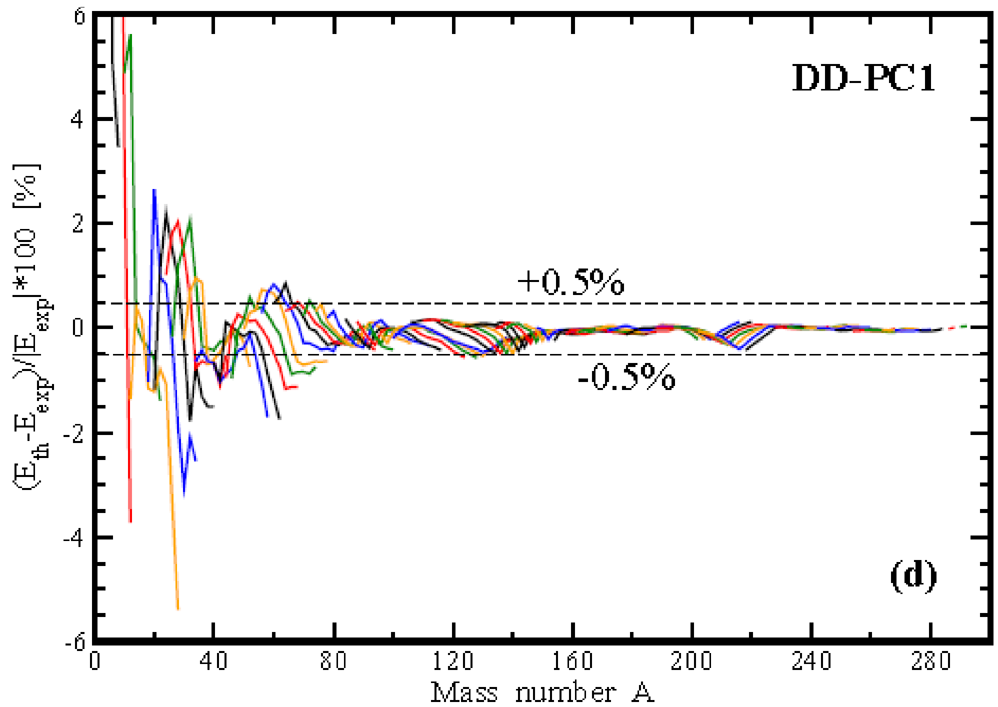

EDF	measured	measured+estimated		
	$\Delta E_{\rm rms}$	$\Delta E_{\rm rms}$	$\Delta(S_{2n})_{\rm rms}$	$\Delta(S_{2p})_{\rm rms}$
NL3*	2.96	3.00	1.23	1.29
DD-ME2	2.39	2.45	1.05	0.95
DD-MEδ	2.29	2.40	1.09	1.09
DD-PC1	2.01	2.15	1.16	1.03

S. Agbemava, AA, D, Ray, P.Ring, PRC **89**, 054320 (2014)
includes complete DD-PC1 mass table as supplement

Uncertainties in radii

CEDF	Δr_{ch}^{rms} [fm]
NL3*	0.0283
DD-ME2	0.0230
DD-MEδ	0.0329
DD-PC1	0.0253

Definition of statistical errors

J. Dobaczewski et al, J. Phys. G, **41** (2014) 074001

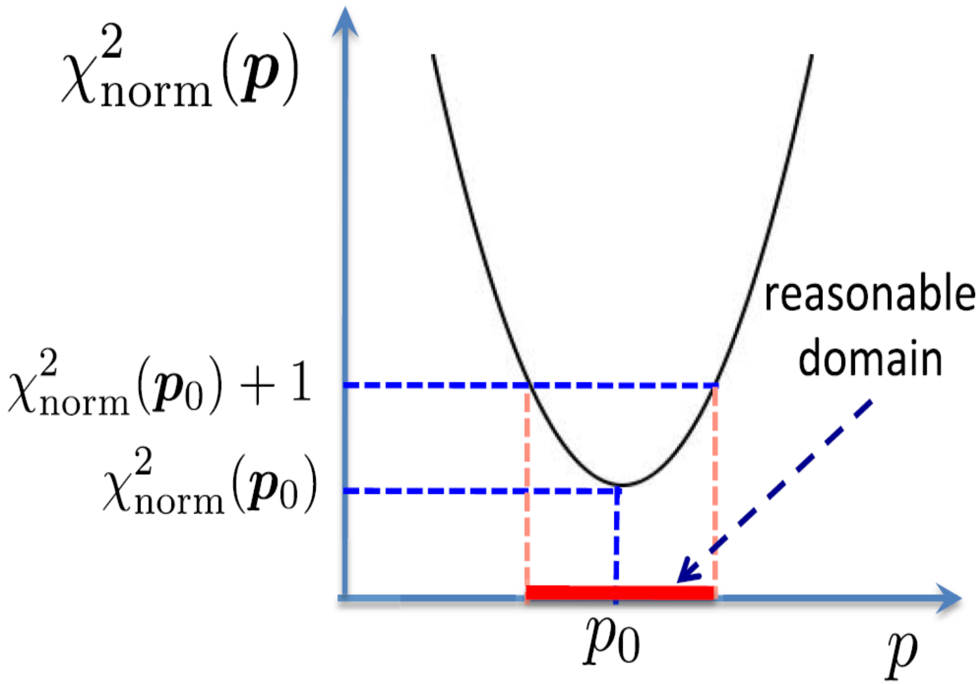

$$\chi^2_{norm}(\mathbf{p}) = \frac{1}{s}\sum_{i=1}^{N_{type}}\sum_{j=1}^{n_i}\left(\frac{O_{i,j}(\mathbf{p}) - O^{exp}_{i,j}}{\Delta O_{i,j}}\right)^2$$

$\mathcal{O}_i(\boldsymbol{p})$ stands for the calculated values

$\mathcal{O}_i^{\text{exp}}$ for experimental data,

$\Delta\mathcal{O}_i$ for adopted errors

$$\Delta\mathcal{O}_i^2 = (\Delta\mathcal{O}_i^{\text{exp}})^2 + (\Delta\mathcal{O}_i^{\text{num}})^2 + (\Delta\mathcal{O}_i^{\text{the}})^2$$

small — small — subjective

$$s = \frac{\chi^2_{norm}(\mathbf{p}_0)}{N_{data} - N_{par}}$$

Birge factor (global scale factor)

For p_i in a "reasonable domain"

$$\sigma = \sqrt{\frac{1}{N}\sum_{i=1}^{N}(O(p_i) - O(p_0))^2}$$

Reexamining the structure of superheavy nuclei in CDFT

Detailed results in S. Agbemava et al, PRC **92**, 054310 (2015)

Covariant density functional theory: Reexamining the structure of superheavy nuclei

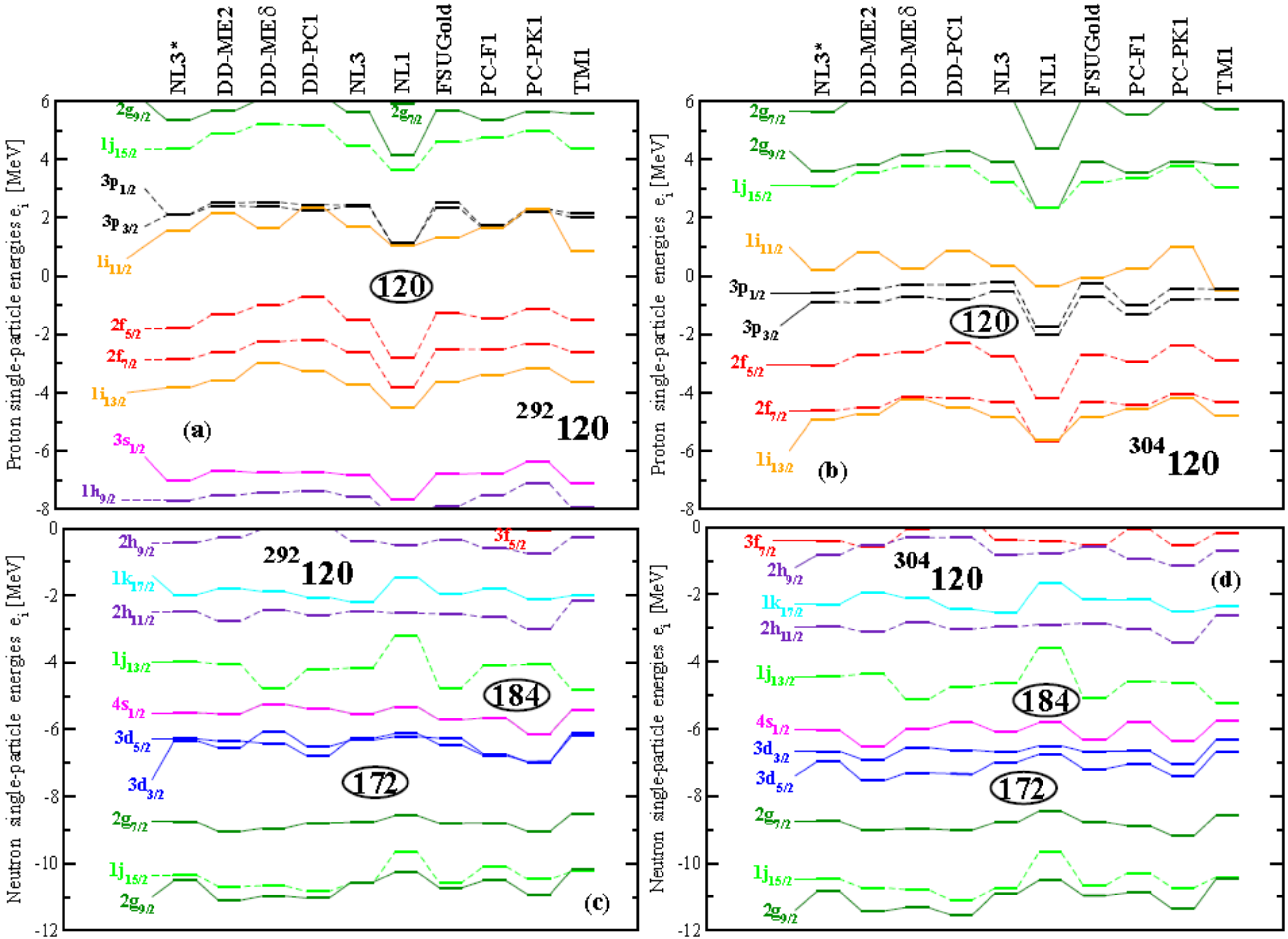
NL3*
DD-ME2
DD-MEδ
DD-PC1
NL3
NL1
FSUGold
PC-F1
PC-PK1
TM1
Proton single-particle energies e_i [MeV]
$2g_{9/2}$
$2g_{7/2}$
$1j_{15/2}$
$3p_{1/2}$
$3p_{3/2}$
$1i_{11/2}$
120
$2f_{5/2}$
$2f_{7/2}$
$1i_{13/2}$
(a)
$^{292}120$
$3s_{1/2}$
$1h_{9/2}$
(b)
$^{304}120$
Neutron single-particle energies e_i [MeV]
$2h_{9/2}$
$3f_{5/2}$
$3f_{7/2}$
$1k_{17/2}$
$2h_{11/2}$
$1j_{13/2}$
184
$4s_{1/2}$
$3d_{5/2}$
$3d_{3/2}$
172
$2g_{7/2}$
$1j_{15/2}$
$2g_{9/2}$
(c)
(d)
6
4
2
0
-2
-4
-6
-8
-10
-12

Deformation effects on shell structure

→ Very important – deformed results differ substantially from spherical ones

Unusual feature: oblate shapes above the spherical shell closures

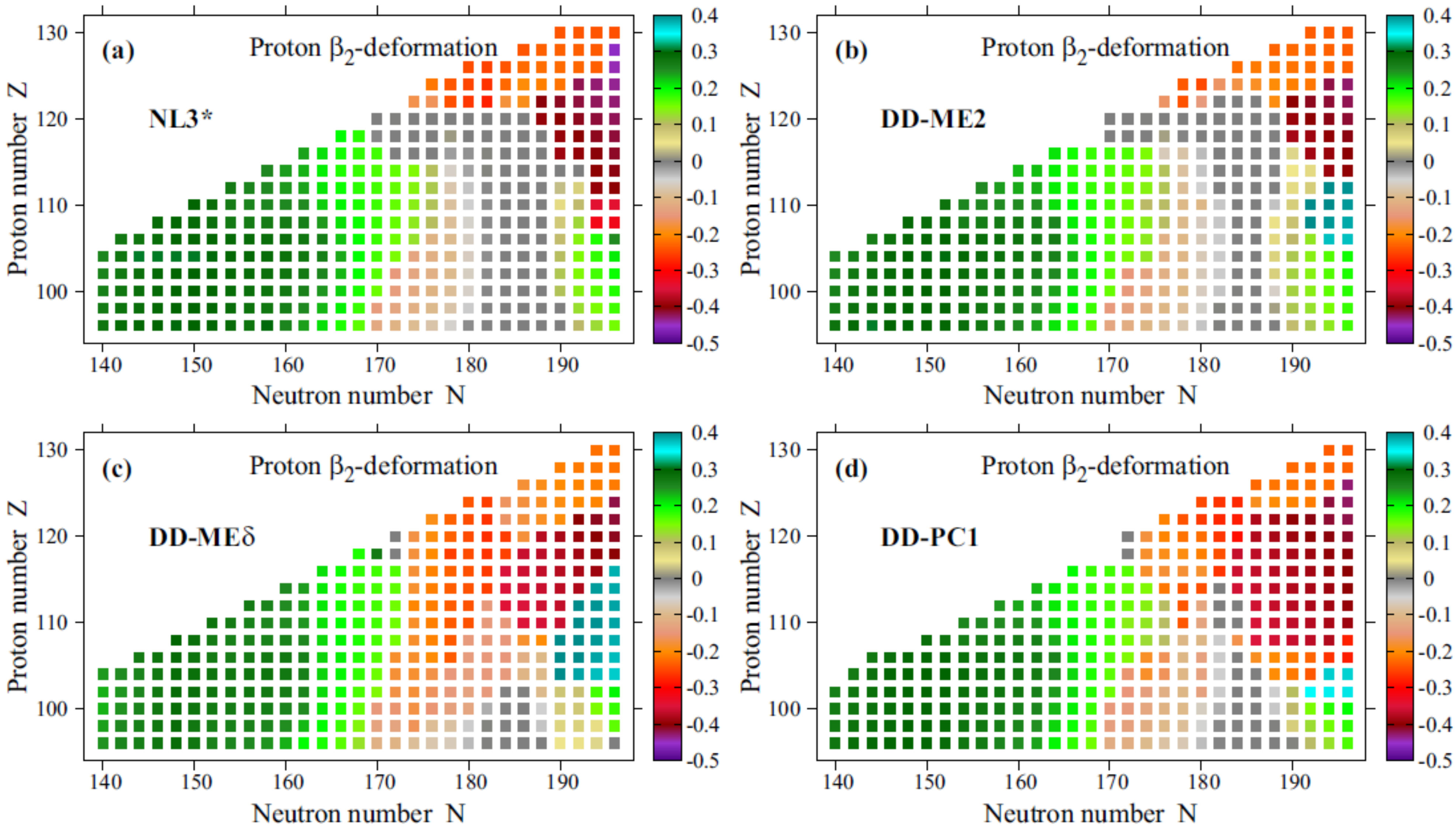

Results for PC-PK1 are very similar to the ones with NL3*

The spreads (theoretical uncertainties) in the deformations

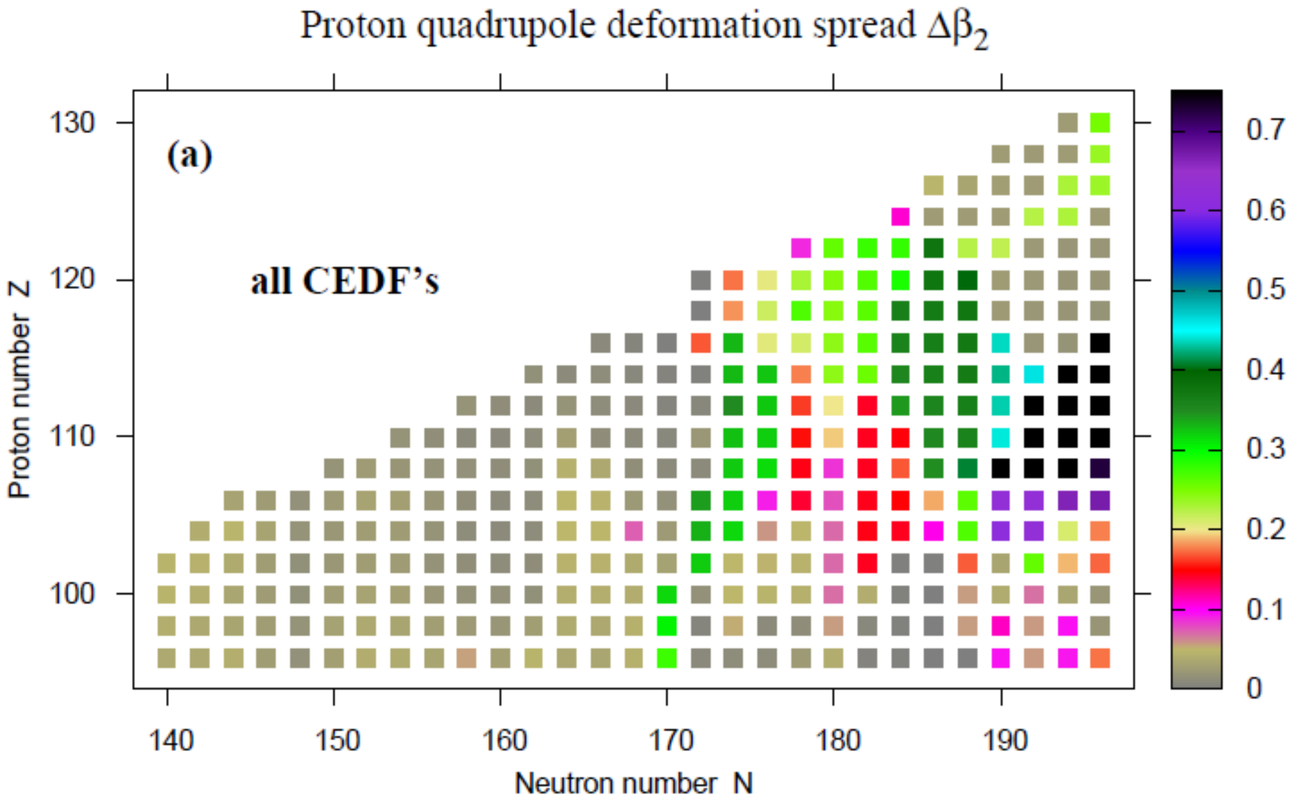

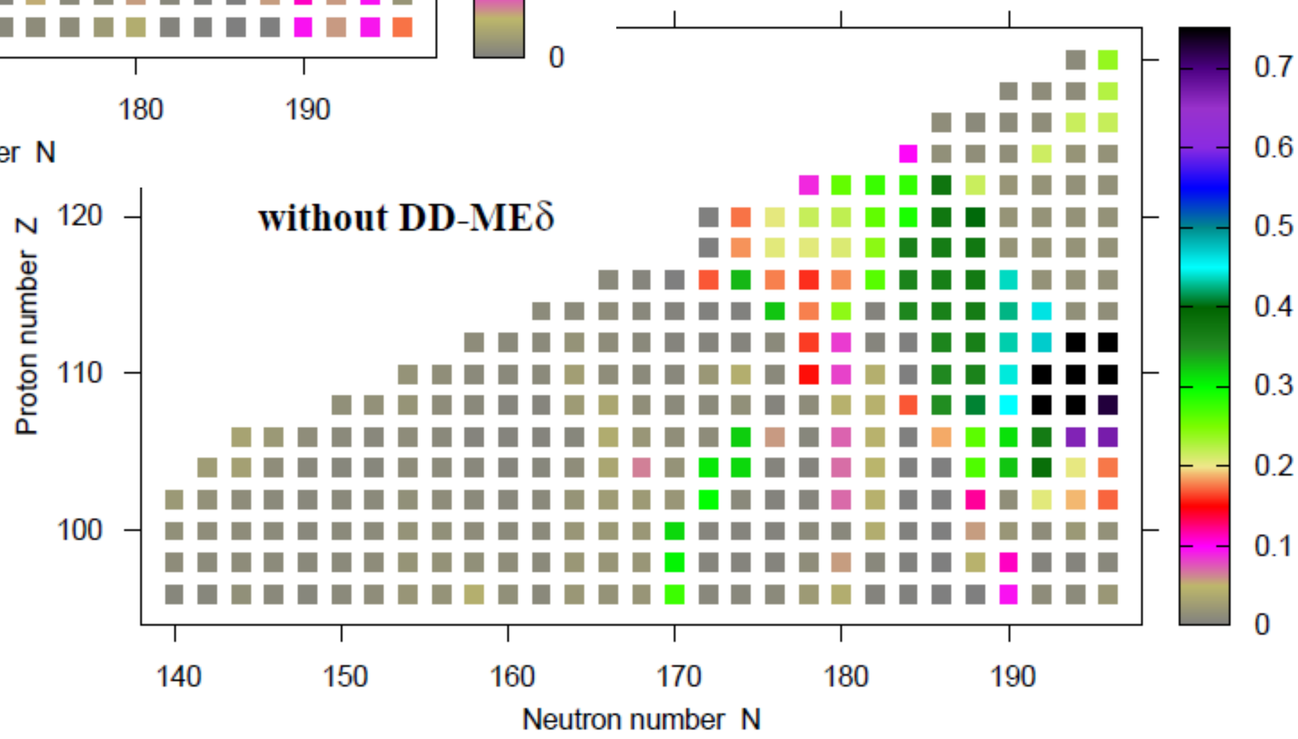

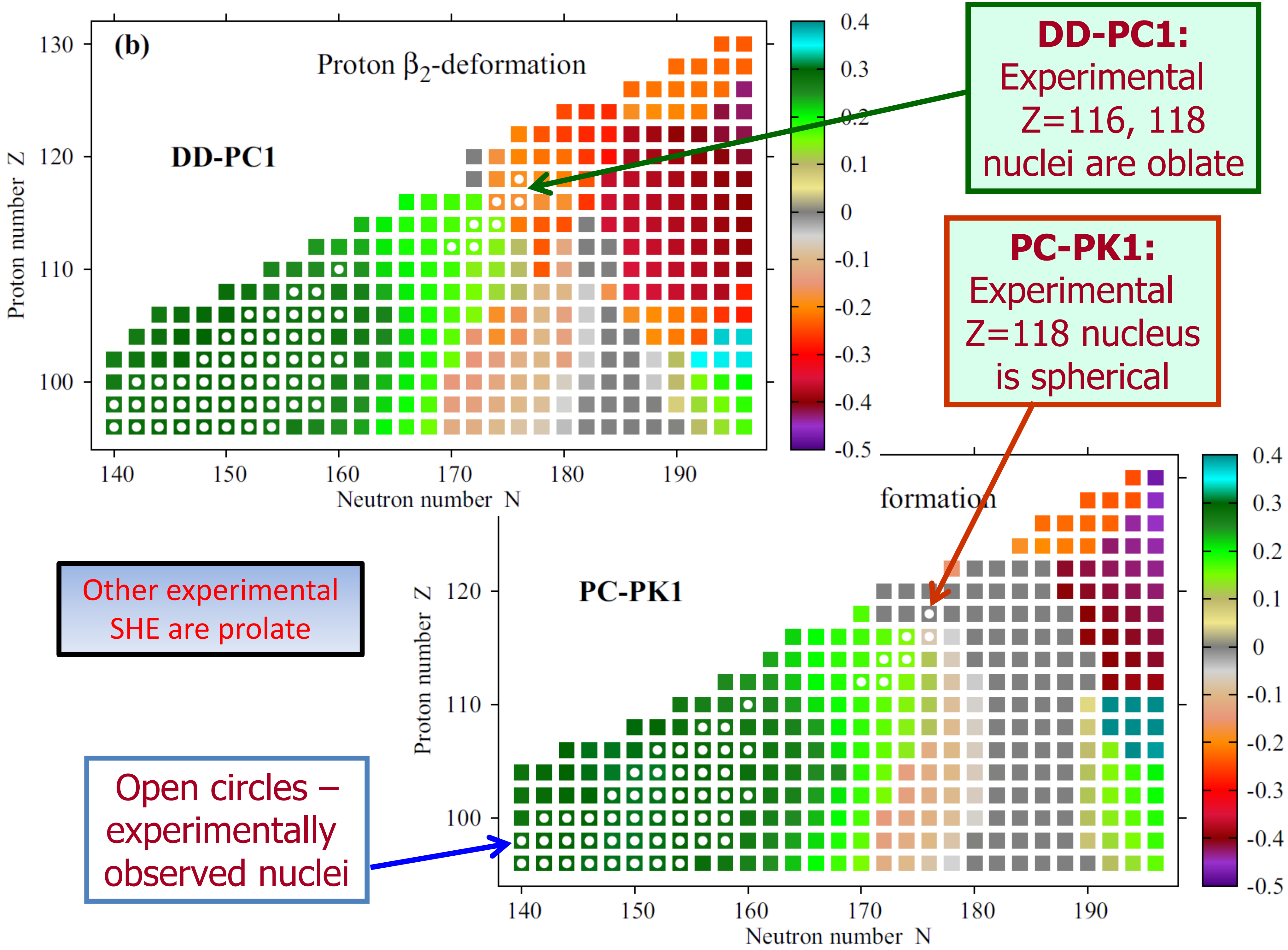

(b)
Proton β2-deformation
DD-PC1
Proton number Z
Neutron number N
DD-PC1:
Experimental
Z=116, 118
nuclei are oblate
PC-PK1:
Experimental
Z=118 nucleus
is spherical
formation
PC-PK1
Proton number Z
Neutron number N
Other experimental
SHE are prolate
Open circles –
experimentally
observed nuclei

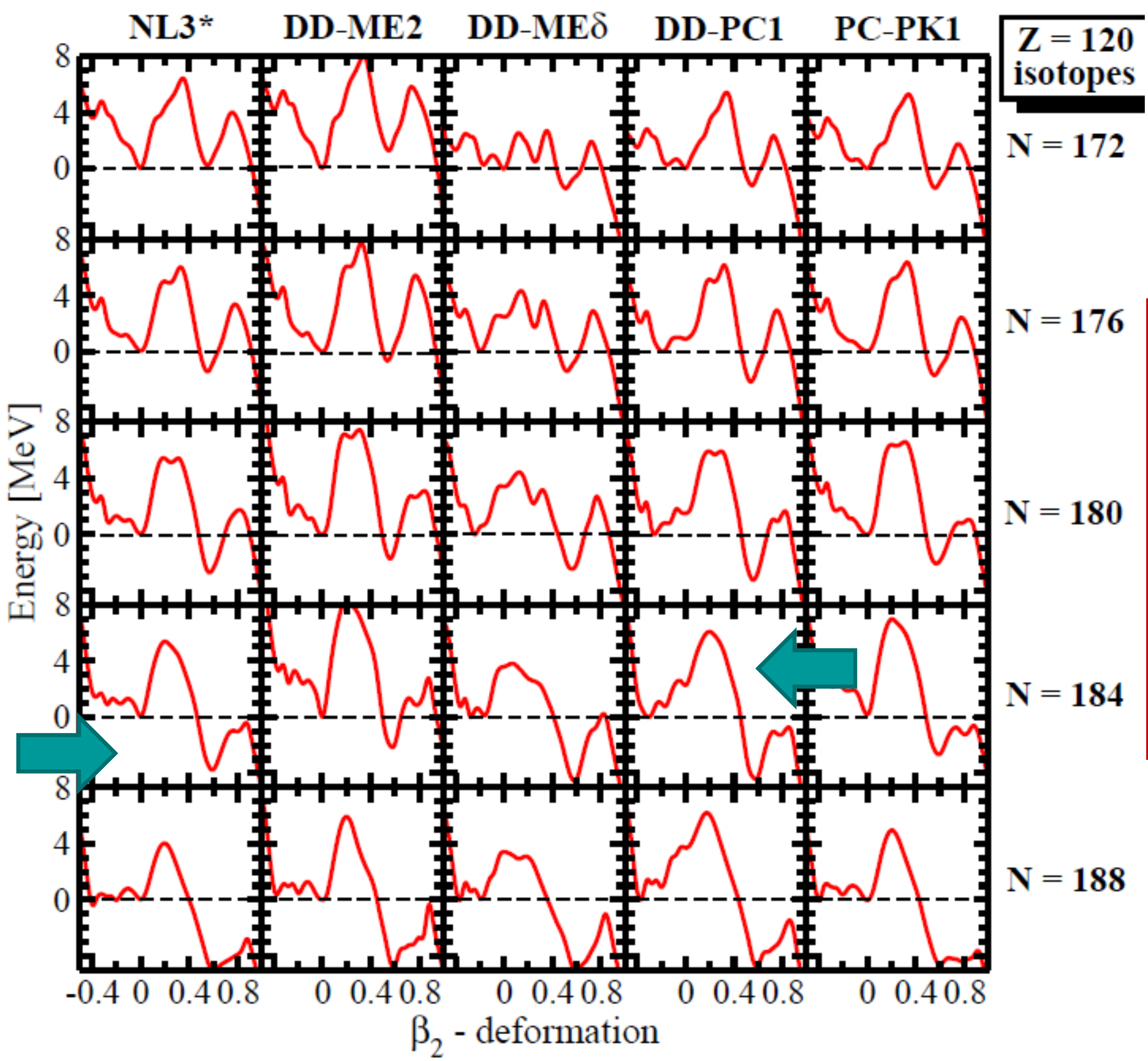

Potential energy surfaces in axially symmetric RHB calculations with separable pairing

The source of oblate shapes – the low density of s-p states

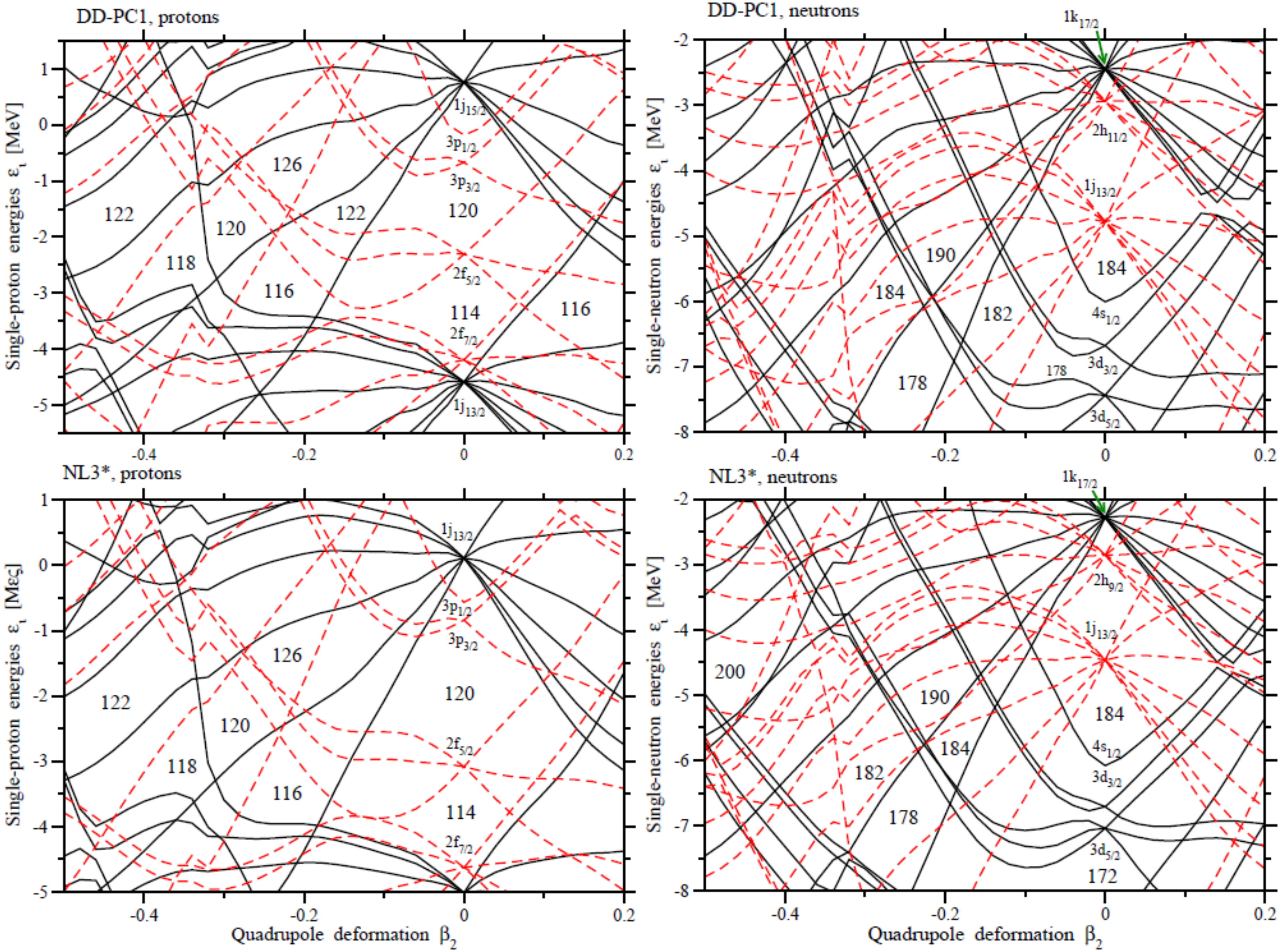

Statistical errors in the description of absolute and relative single-particle energies.

Neutron			Proton		
Orbital	$\bar{e}_\nu$	$\sigma(e_\nu)$	Orbital	$\bar{e}_\pi$	$\sigma(e_\pi)$
$4s_{1/2}$	-6.091	0.209	$2f_{5/2}$	-2.981	0.334
Neutron Fermi level			Proton Fermi level		
$1j_{13/2}$	-4.536	0.280	$3p_{3/2}$	-0.818	0.332

Neutron			Proton		
Orbital pairs (m, j)	$\overline{\Delta e_\nu}$	$\sigma(\Delta e_\nu)$	Orbital pairs (m, j)	$\overline{\Delta e_\pi}$	$\sigma(\Delta e_\pi)$
$3d_{5/2}$ - $3d_{3/2}$	0.305	0.007	$1i_{13/2}$ - $2f_{7/2}$	0.309	0.019
$3d_{3/2}$ - $4s_{1/2}$	0.628	0.008	$2f_{7/2}$ - $2f_{5/2}$	1.550	0.024
below neutron Fermi level			below proton Fermi level		
$4s_{1/2}$ - $1j_{13/2}$	1.554	0.121	$2f_{5/2}$ - $3p_{3/2}$	2.163	0.033
$1j_{13/2}$ - $2h_{11/2}$	1.527	0.102	$3p_{3/2}$ - $3p_{1/2}$	0.314	0.005

$$\Delta e_i(m, j) = e_i(m) - e_i(j)$$

Confronting experimental data

E. Litvinova, AA, PRC 84, 014305 (2011)

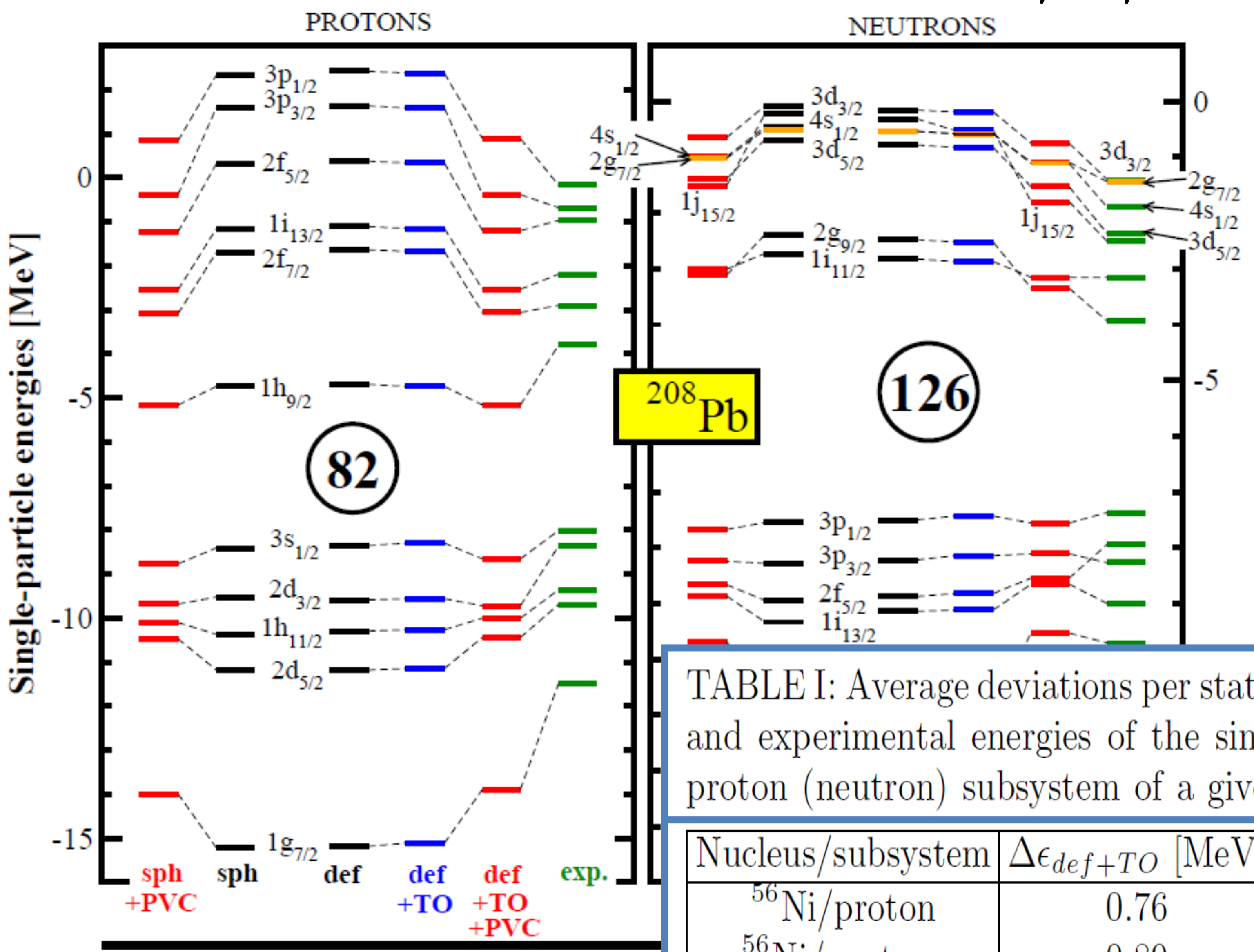

NL3* functional

particle-vibration coupling
+ TO, TE polarization effects

TABLE I: Average deviations per state $\Delta\epsilon$ between calculated and experimental energies of the single-particle states for a proton (neutron) subsystem of a given nucleus. The results

Nucleus/subsystem	$\Delta\epsilon_{def+TO}$ [MeV]	$\Delta\epsilon_{def+TO+PVC}$ [MeV]
^{56}Ni/proton	0.76	0.77
^{56}Ni/neutron	0.89	0.71
^{132}Sn/proton	1.02	0.68
^{132}Sn/neutron	0.89	0.39
^{208}Pb/proton	1.53	0.84
^{208}Pb/neutron	1.00	0.47

Statistical distribution of deviations of the energies of one-quasiparticle states from experiment

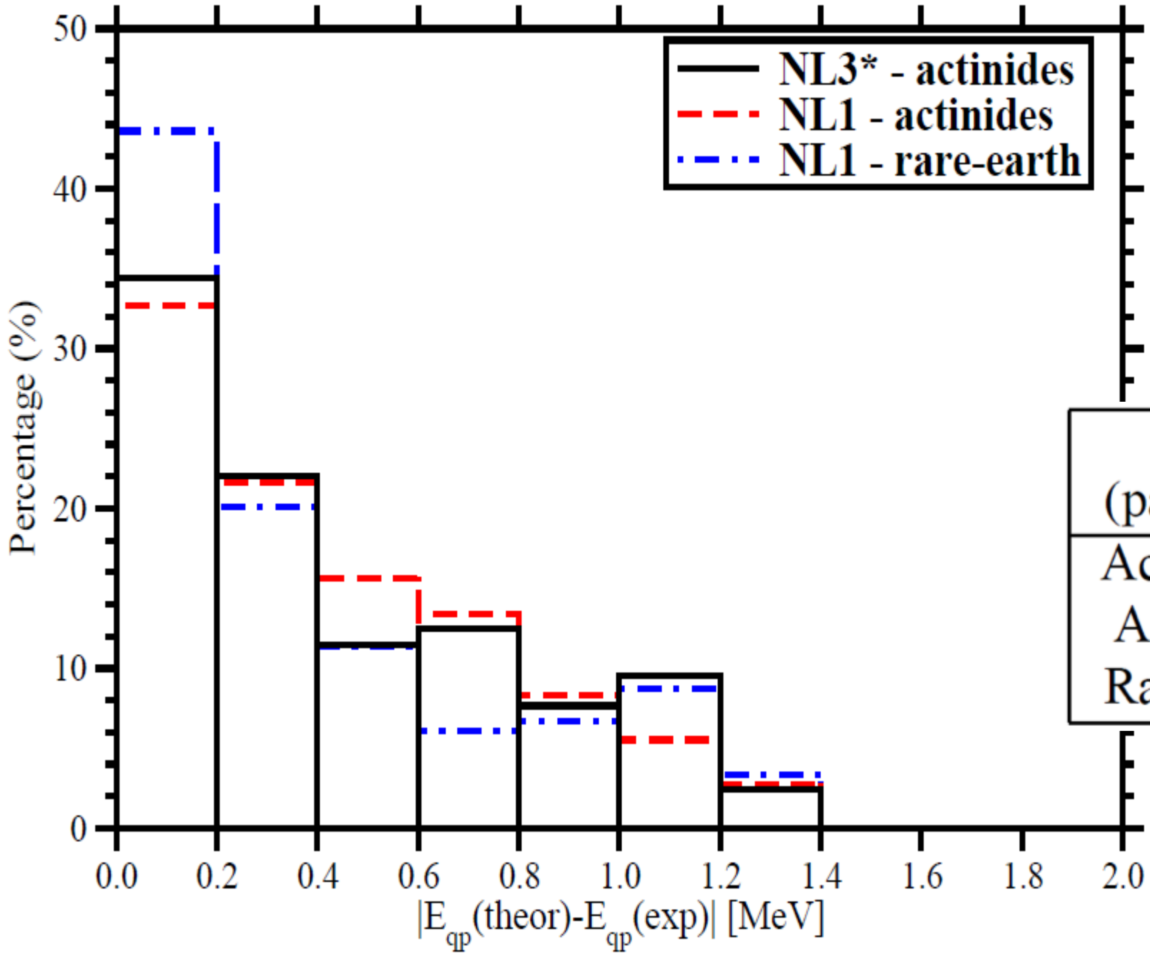

The description of deformed states at DFT level is better than spherical ones by a factor 2-3 (and by a factor ~1 (neutron) and ~2 (proton) as compared with spherical PVC calculations)

Region (parametrization)	calculated states (#)	compared states (#)
Actinides (NL3*)	415	209
Actinides (NL1)	444	217
Rare-earth (NL1)	360	149

Triaxial CRHB; fully self-consistent blocking, time-odd mean fields included, NL3*, Gogny D1S pairing,
AA and S.Shawaqfeh,
PLB 706 (2011) 177

Two sources of deviations:

1. Low effective mass (stretching of the energy scale)
2. Wrong relative energies of the states

Similar problems in Skyrme and Gogny DFT

Deformed one-quasiparticle states: covariant and non-relativistic DFT description versus experiment

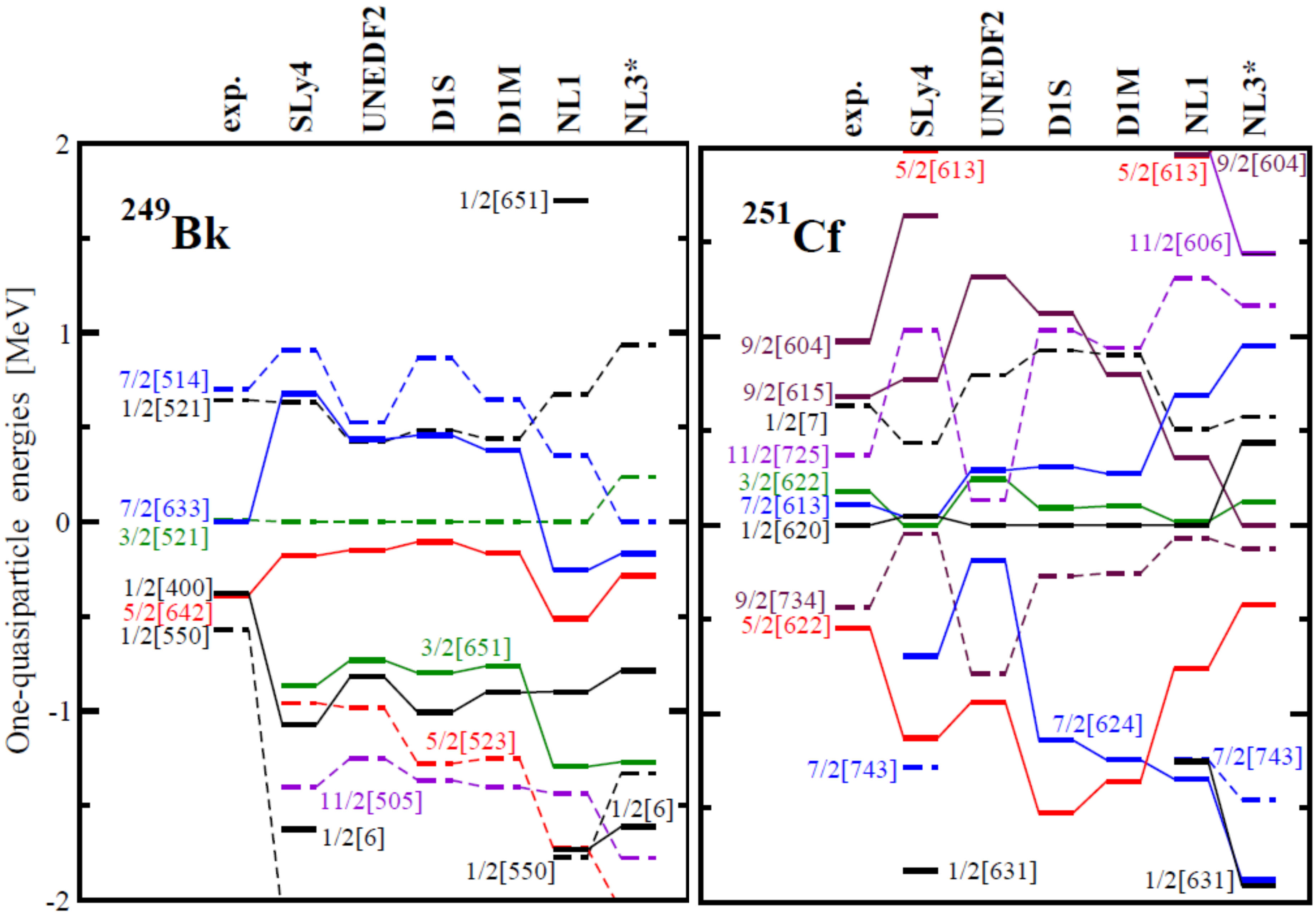

J.Dobaczewski, AA, M.Bender, L.M.Robledo, Yue Shi, NPA 944 (2015) 388

Accuracy of the description of experimental data in Z>94 nuclei

CEDF	ΔE_{rms} [MeV]	$\Delta(S_{2n})_{rms}$ [MeV]	$\Delta(S_{2p})_{rms}$ [MeV]	$\Delta(Q_\alpha)_{rms}$ [MeV]
1	2	3	4	5
NL3*	3.02/3.39	0.71/0.68	1.33/1.34	0.68/0.75
DD-ME2	1.39/1.40	0.45/0.54	0.85/0.90	0.51/0.65
DD-MEδ	2.52/2.45	0.60/0.51	0.45/0.48	0.39/0.51
DD-PC1	**0.59/0.74**	0.30/0.32	0.41/0.42	0.36/0.47
PC-PK1	2.82/2.63	**0.25/0.23**	**0.36/0.33**	**0.32/0.38**

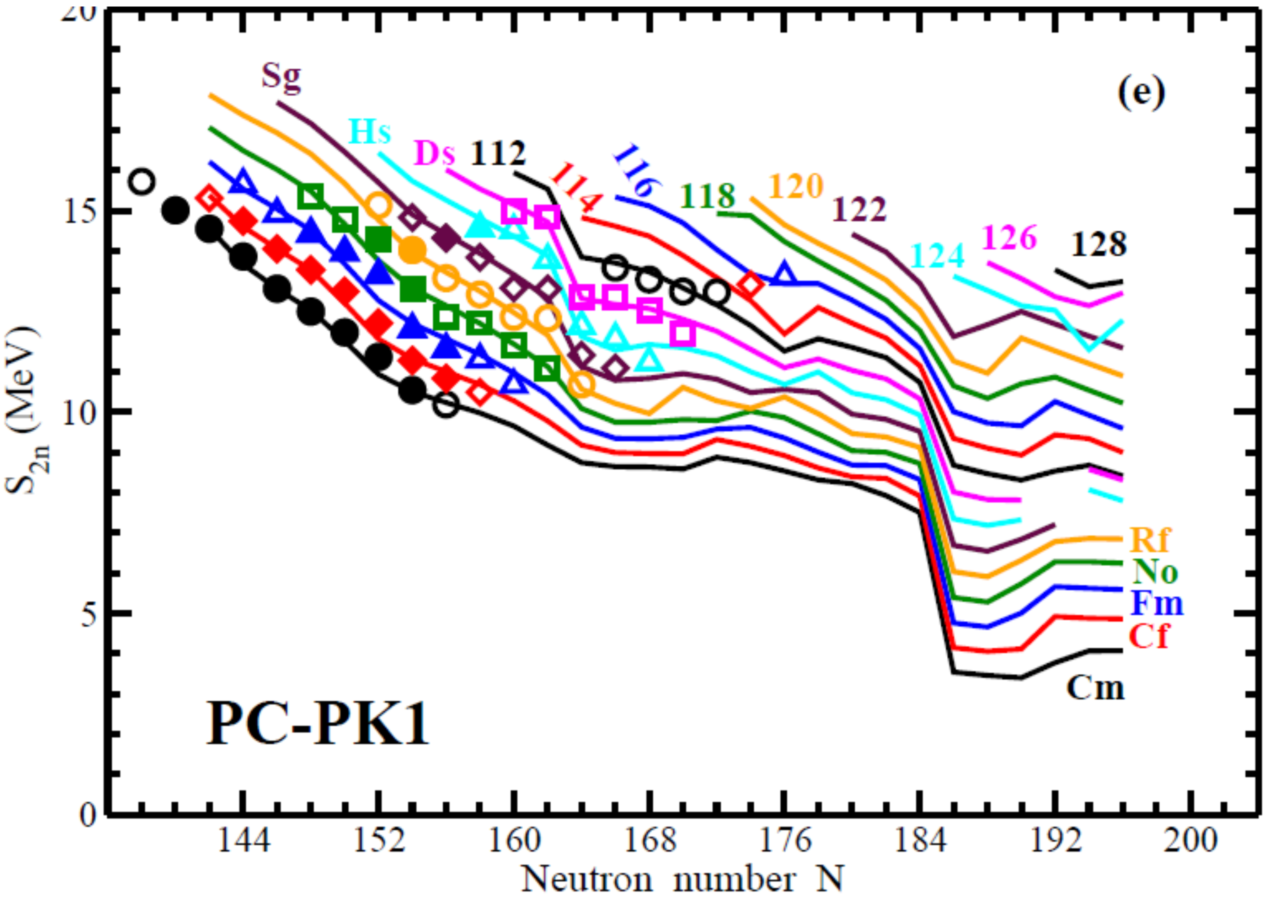

With exception of the DD-MEδ, the deformed N=162 gap is well reproduced in all CEDF's

The Q_α-values

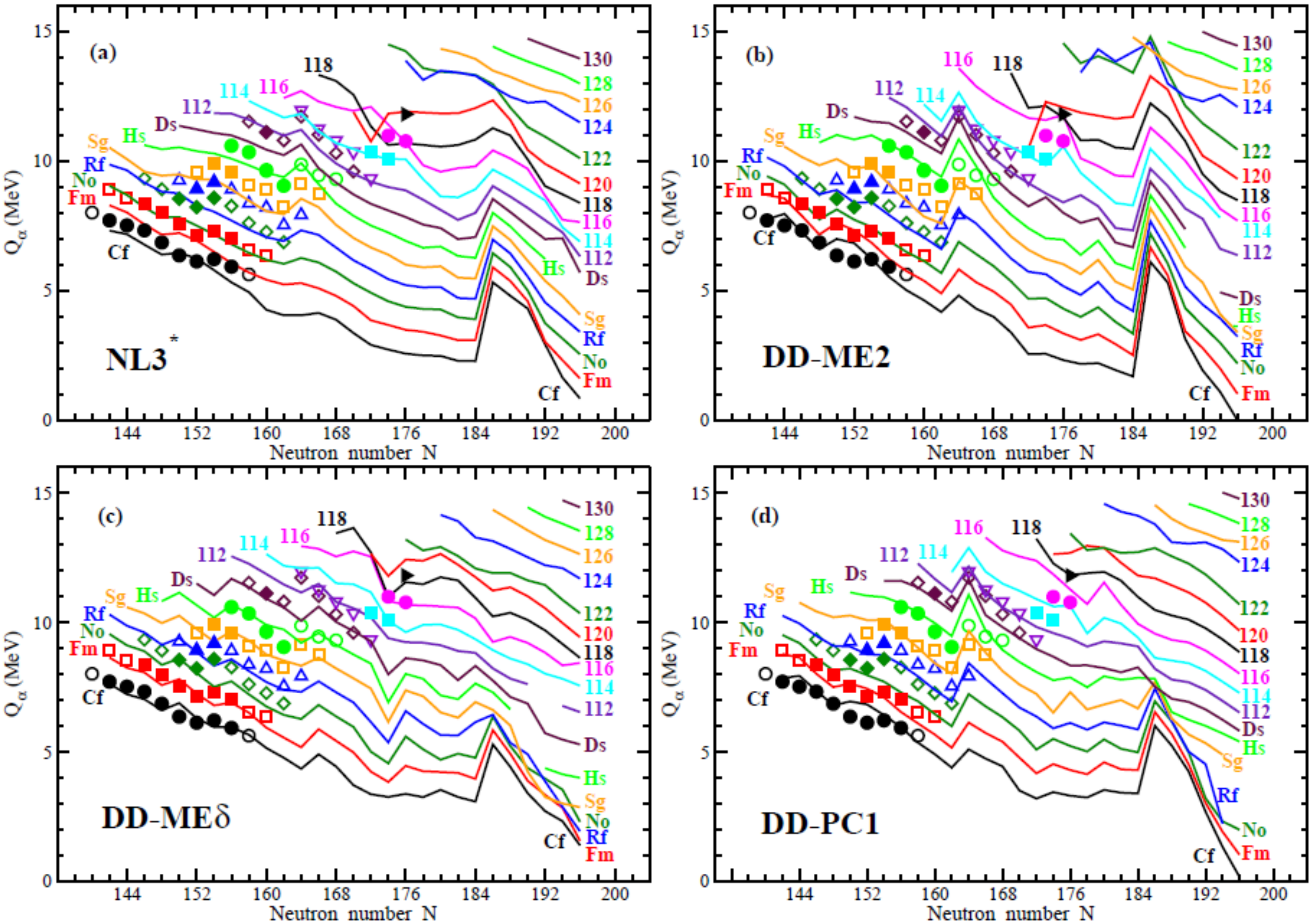

Fission barriers: theory versus experiment [state-of-the-art]

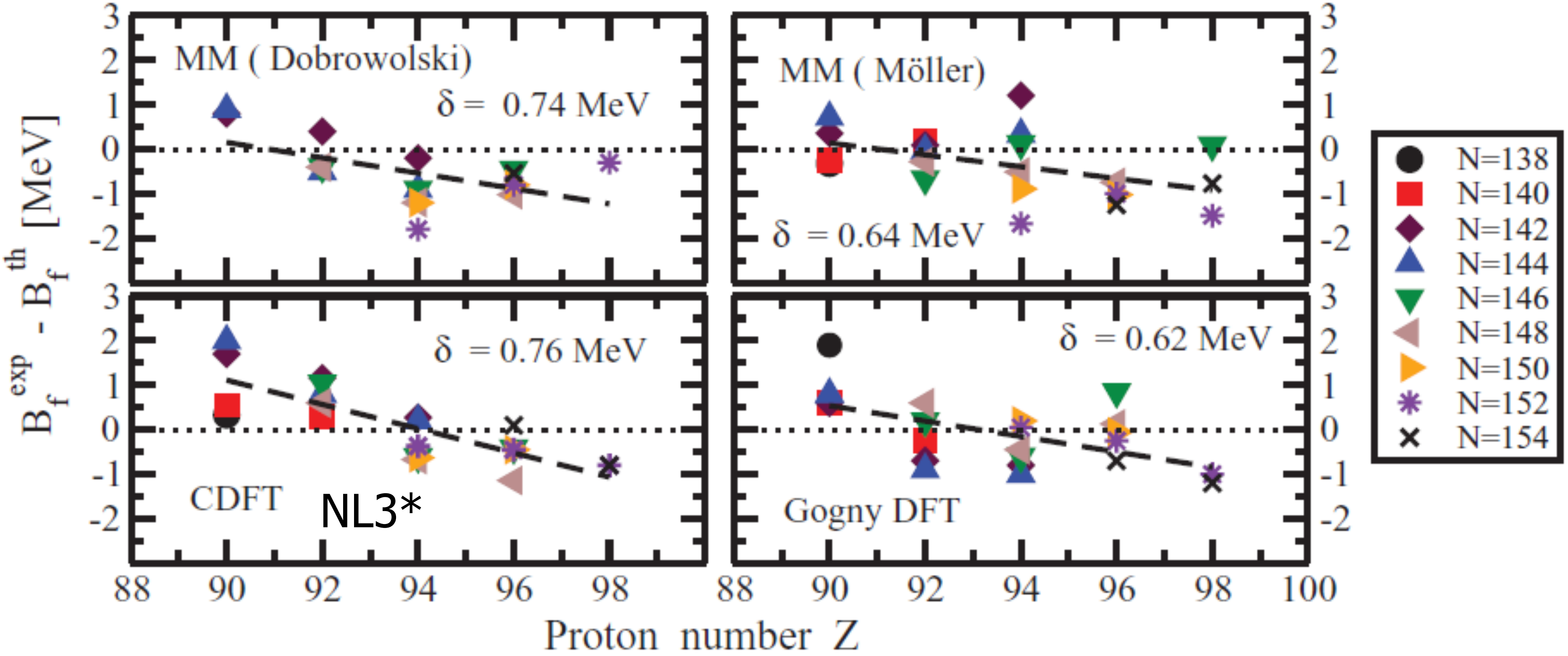

Mac+mic, LSD model
A.Dobrowolski et al,
PRC 75, 024613 (2007)

Mac+mic, FRDM model
P. Moller et al,
PRC 79, 064304 (2009)

Gogny DFT,
J.-P. Delaroche et al,
NPA 771, 103 (2006).

CDFT : actinides H. Abusara, AA and P. Ring, PRC 82, 044303 (2010)
superheavies: H. Abusara, AA and P. Ring, PRC 85, 024314 (2012)

No fit of functionals (parameters) to fission barriers or fission isomers
only in mac+mic (Kowal) and CDFT

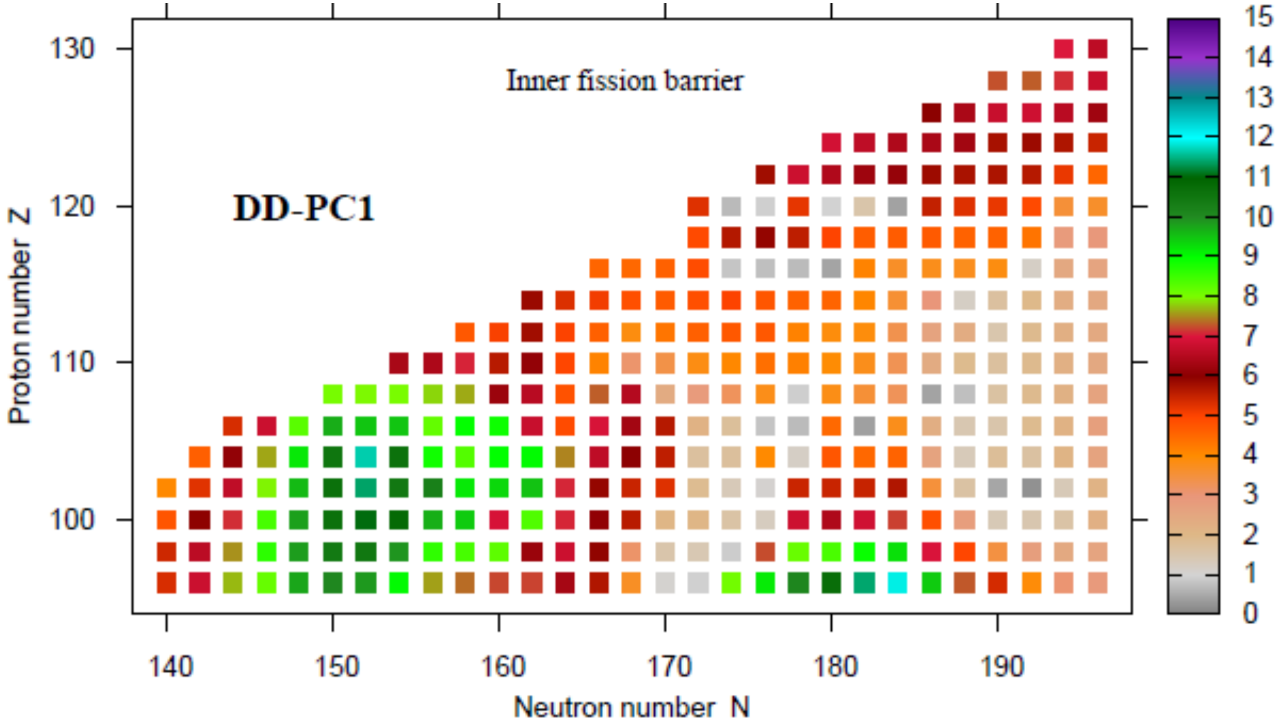

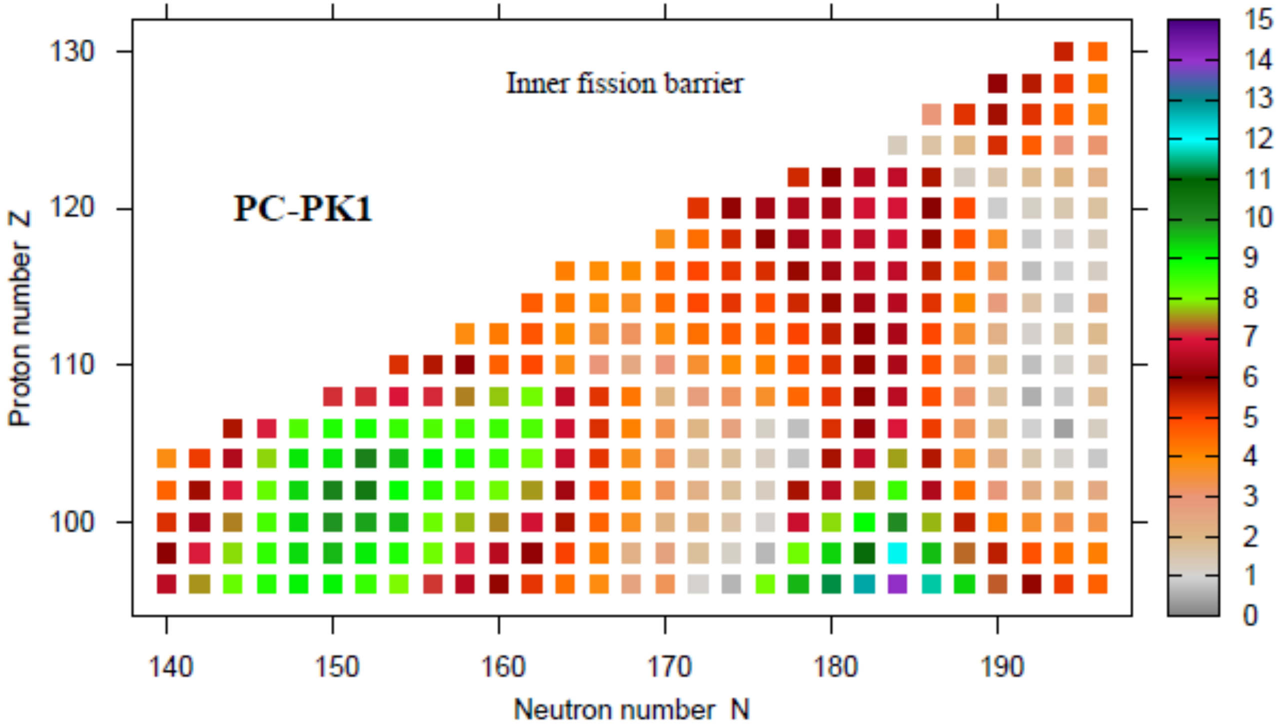

Inner fission barrier heights as obtained in axially symmetric RHB with separable pairing

provides upper limit for inner barrier height

The spreads (theoretical uncertainties) in the heights of inner fission barriers in superheavy nuclei

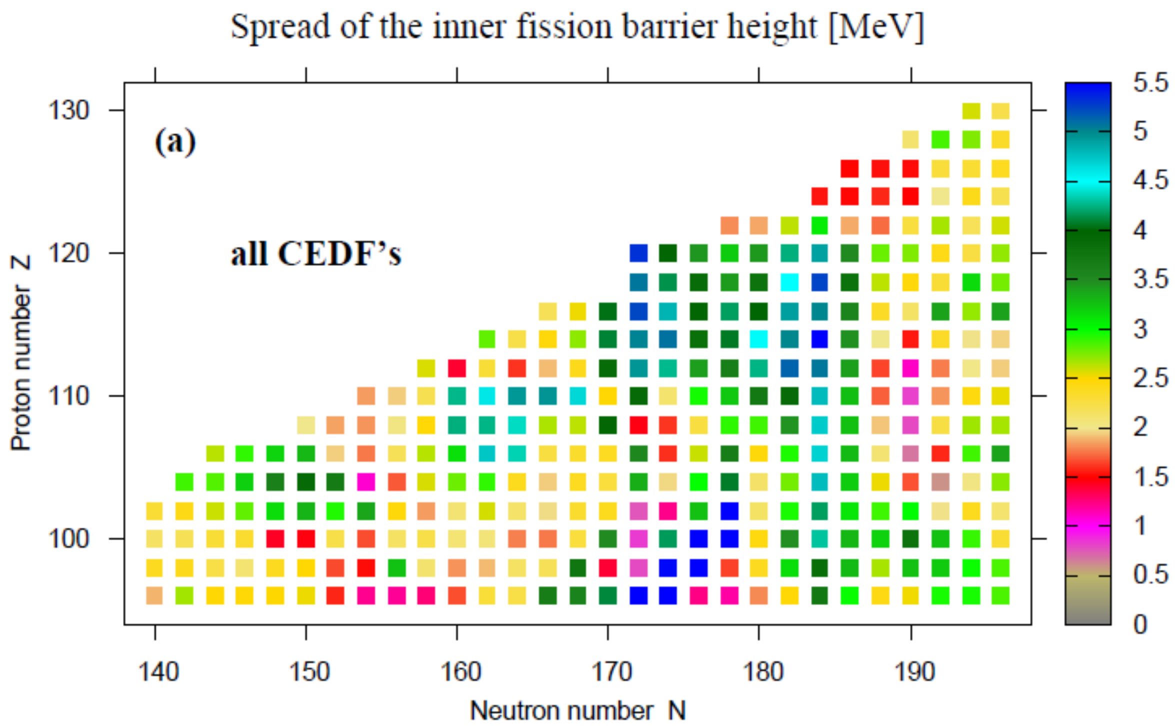

Axial RHB calculations

Benchmarking of fission barriers in actinides (done for NL3*, DD-PC1 and PC-PK1) reduces theoretical uncertainties and makes the description of fission barriers more predictive

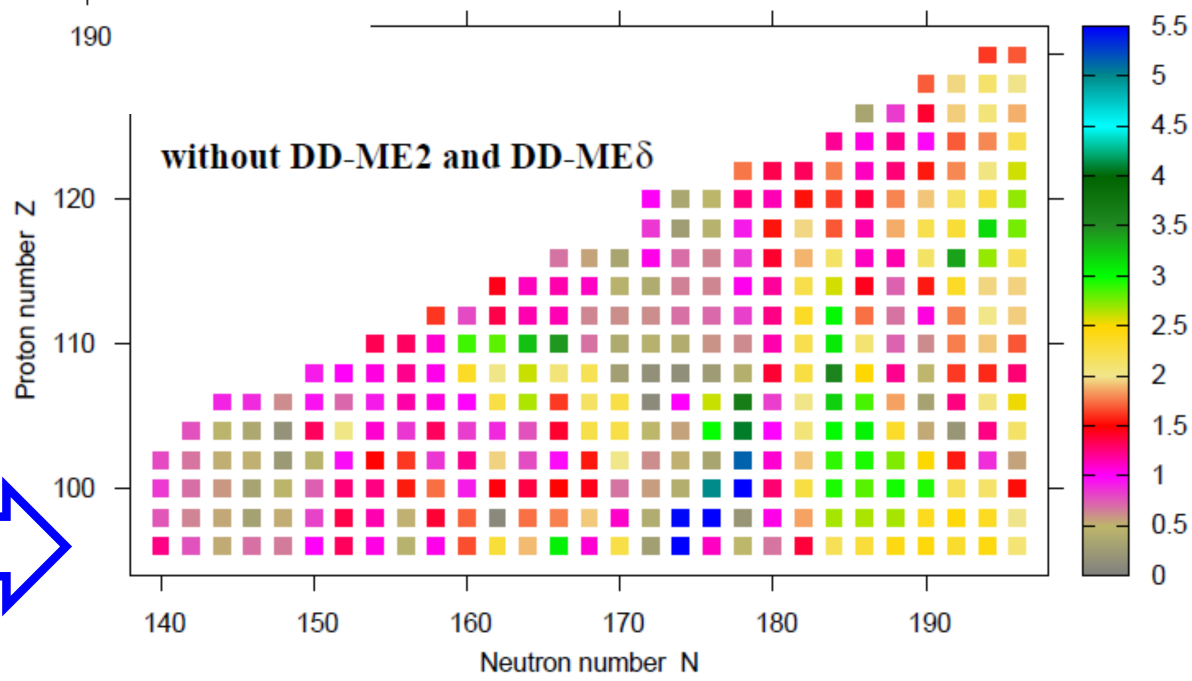

The impact of triaxiality on inner fission barriers in SHE

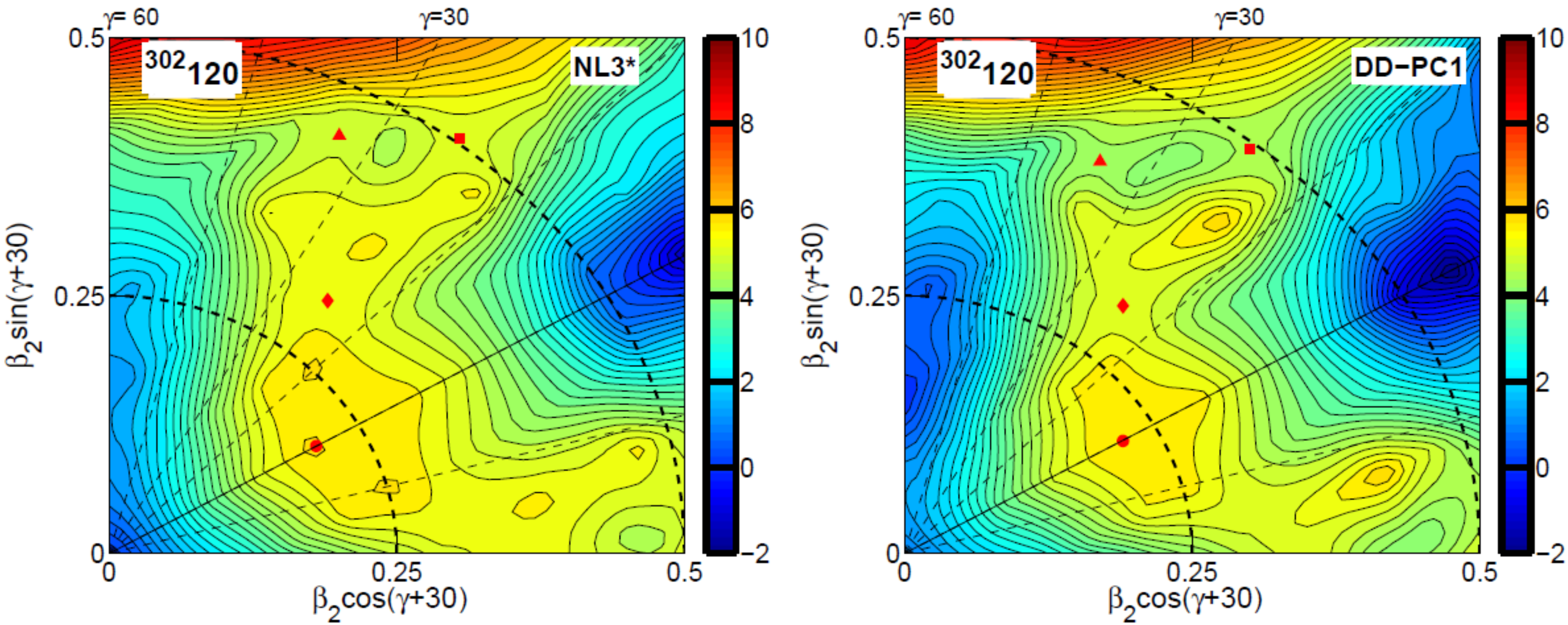

Spreads of the inner fission barrier heights [MeV]

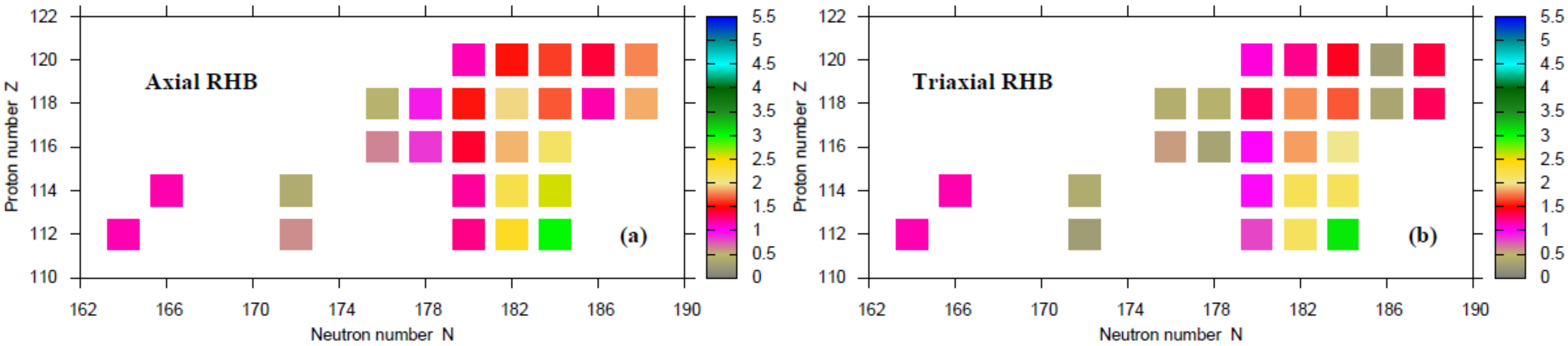

The heights of inner fission barriers in superheavy nuclei

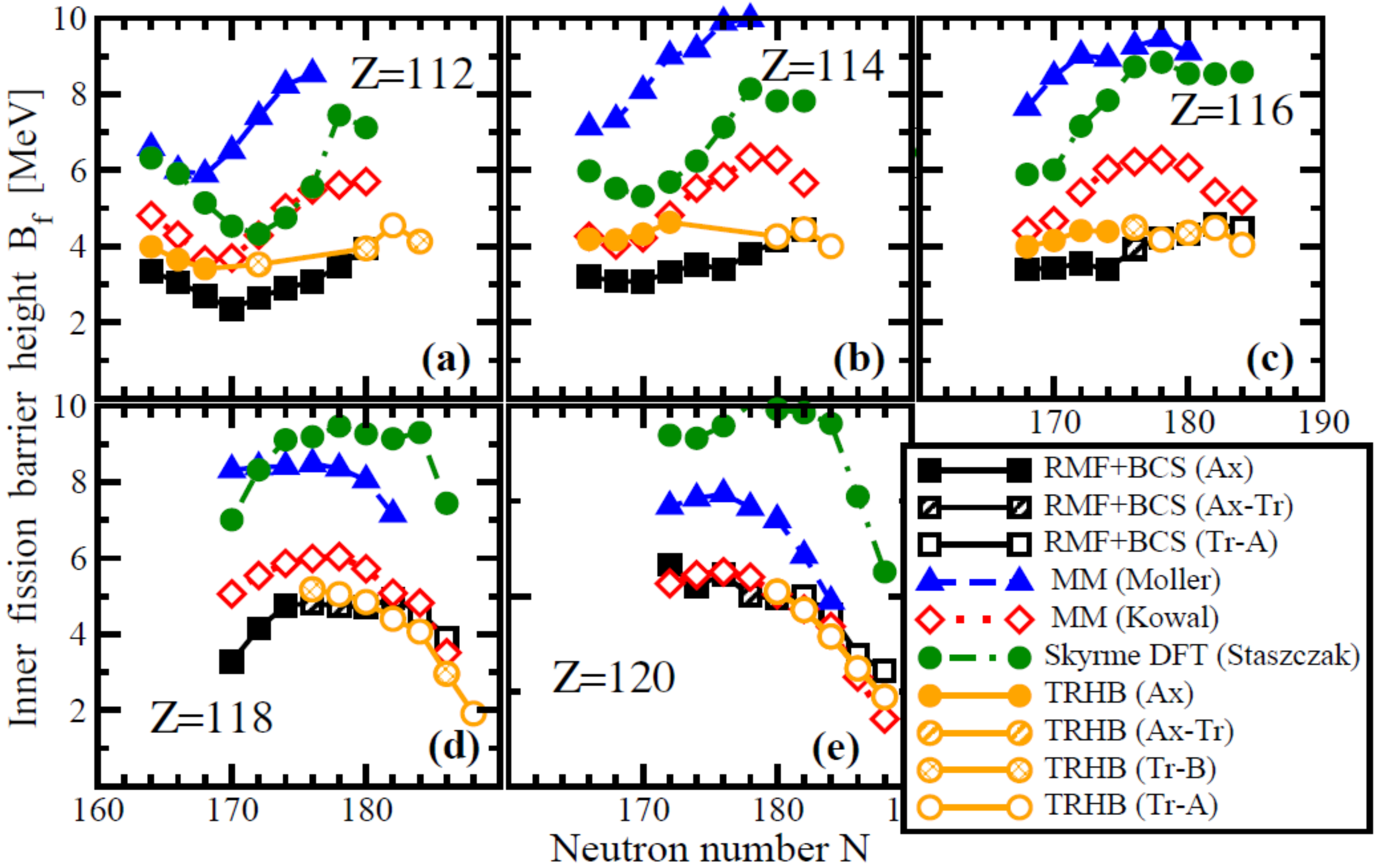

A. Staszczak et al, PRC 87, 024320 (2013) – Skyrme SkM*
M. Kowal et al, PRC 82, 014303 (2010) – WS pot. + Yukawa exponent. model
P. Moller et al, PRC 79, 064304 (2009) – folded Yukawa pot. + FRDM model

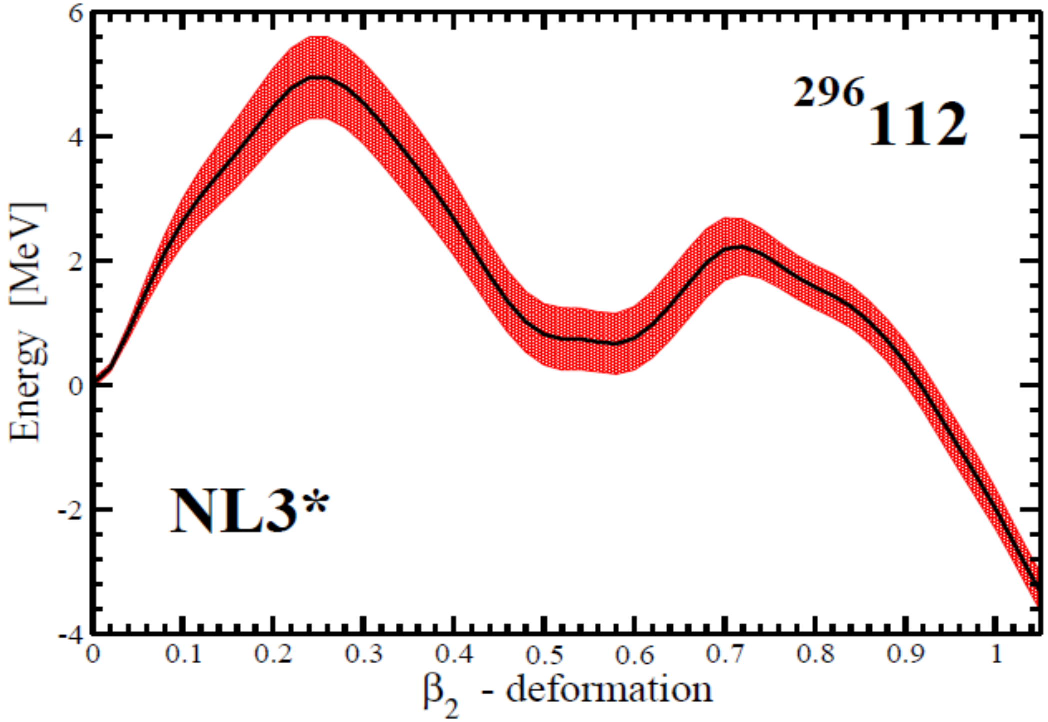

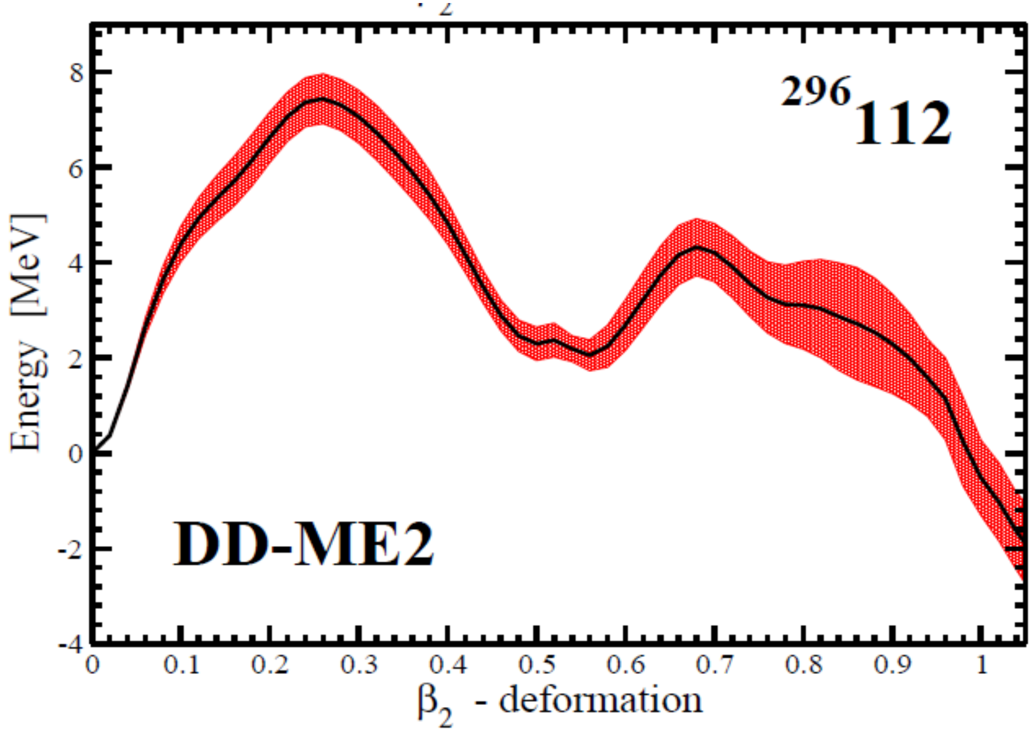

Statistical uncertainties in the description of potential energy curves and fission barriers

Black curve – mean value of the energy, close to the energy of the optimal functional

The red colored region shows the standard deviations in energy

Increased statistical uncertainties at some deformations are due to underlying single-particle structure

Conclusions

1. The accuracy of the description and theoretical uncertainties have been quantified for
   - **deformations** [PRC 88, 014320 (2013) and PRC 92,054310 (2015)]
   - masses, separation energies [PRC 89, 054320 (2014), 92, 054310 (2015)]
   - **α-decays** [PRC 92,054310 (2015)]
   - **fission barriers** [PLB 689, 72 (2010), PRC 82, 044303 (2010), PRC 85, 024314 (2012), new man. subm. to PRC]
   - **single-particle energies** [PRC 84, 014305 (2011), PLB 706, 177 (2011), NPA 944, 388 (2015)]
   - moments of inertia [PRC 88, 014320 (2013), Phys. Scr. 89, 054001 (2014)]
   - **pairing** [PRC 88, 014320 (2013) and PRC 89, 054320 (2014)]

   in actinides and superheavy nuclei.

2. **Detailed analysis with deformation included does not confirm the importance of the N=172 spherical shell gap**. On the contrary, a number of functionals show important role of the N=184 shell gap.

3. Some functionals do not predict spherical SHE around Z=120 and N=184 lines !!!

Conclusions

4. Available experimental data in actinides and SHE does not allow to give a clear preference to a specific functional predictions in the Z~120, N~184 region.

5. Fission barriers: systematic theoretical uncertainties and statistical errors for inner fission barriers of SHE within the CDFT framework have been estimated. The differences between the models in the fission barrier heights in SHE are substantial.

This material is based upon work supported by the U.S. Department of Energy, Office of Science, Office of Nuclear Physics under Award No. DE-SC0013037 and National Nuclear Security Administration under Award No. DE-NA0002925